PCCP

Dissociative Electron Attachment induced Ring Opening in Five-Membered Heterocyclic Compounds

Journal:	*Physical Chemistry Chemical Physics*
Manuscript ID	CP-ART-04-2018-002718.R1
Article Type:	Paper
Date Submitted by the Author:	06-Jun-2018
Complete List of Authors:	Li, Zhou; University of Notre Dame, Radiation Laboratory and Dept. of Physics Carmichael, Ian; University of Notre Dame, Radiation Laboratory and Department of Chemistry & Biochemistry Ptasinska, Sylwia; University of Notre Dame, Radiation Laboratory and Dept. of Physics

Dissociative Electron Attachment induced Ring Opening in Five-Membered Heterocyclic Compounds

Zhou Li[1,2] *Ian Carmichael*[1], *and Sylwia Ptasińska*[1,2*]

[1]Radiation Laboratory, University of Notre Dame, Notre Dame, IN 46556, USA

[2]Department of Physics, University of Notre Dame, Notre Dame, IN 46556, USA

*corresponding author: sptasins@nd.edu

Abstract

Five-membered heterocyclic structures, which exist widely in biological systems and play an active role in various biochemical processes, have been studied extensively from a fundamental perspective. Here, the fragmentation patterns of isoxazole, a representative five-membered heterocycle, upon dissociative electron attachment (DEA) were examined carefully by comparing isoxazole's products with those of its methylated derivatives. It was found that the most dominant DEA pathway occurs through the loss of hydrogen at C(3), which leads to ring opening by O-N bond cleavage at an energy of ~1.5 eV. The ring opening was investigated further for DEA to other related five-membered ring compounds, *i.e.*, oxazole and thiazole. The DEA-induced hydrogen loss was much less pronounced or quenched completely in these two compounds and simultaneous ring-opening behavior was not detected. This observation is of special interest to applied fields, for example, the pharmaceutical industry, because several drugs that contain isoxazole substructures exhibit extensive ring opening during biotransformation.

I. Introduction

Five-membered aromatic heterocyclic compounds are biologically important and are prevalent in nature. For example, they are present as nucleic acid building units, *i.e.*, the nucleobases adenine and guanine. In recent decades, many heterocyclic biological compounds have been investigated extensively by physical methods to elucidate the effects of radiation at the molecular level, with a particular emphasis on low-energy electron collision processes [1]. Low-energy electrons (LEEs), largely those with an energy below 20 eV that are produced in biological tissue by ionizing radiation, are known to contribute to radiation damage of DNA [2],[3]. Ionizing radiation is used widely in cancer therapy, where its interaction produces showers of low-energy electrons, creating an electron-rich local environment within irradiated living cells. Thus, knowledge of the interaction between LEEs and biomolecules is essential to obtain a full picture of the processes radiation induces in living cells to improve radiotherapeutical outcomes and enhance pharmaceutical engineering technologies. These heterocyclic molecules can be regarded as simple prototypes of more complex biological systems, such as the polynucleotide strands of DNA, and thus, they have been investigated already in several electron-scattering studies [4]–[11]. In addition to their structural function, these compounds also play an important role in various biochemical processes. Structure-activity relation studies [12] have demonstrated that incorporation of one or more heteroatoms in an aromatic ring can significantly alter the chemical and biochemical reactivity and change the subsequent metabolism pathway. Instances have been reported in which medicines that contain aromatic heterocyclic rings were found to induce toxic events and related idiosyncratic autoimmune reactions and thereby were withdrawn from clinical use [13],[14].

In this work, we focused on isoxazole, which is a five-membered aromatic heterocycle that contains two heteroatoms. Isoxazole can be derived from furan by replacing one of the methine (-CH) groups with a nitrogen atom, as shown in Figure 1. The substitution of nitrogen causes a significant change in the compound's properties. For example, compounds that contain an isoxazole substructure have been reported to undergo extensive ring opening through biotransformation [15],[16]. One of the mechanisms proposed is that the greater electronegativity of the oxygen atom adjacent to the nitrogen in the isoxazole ring results in facile reductive cleavage of the N-O bond [17]. Some studies of isoxazole's ring opening mechanism have been conducted previously [17], but none has been performed on fragmentation induced by dissociative electron attachment (DEA).

Although a previous study that used electron transmission spectroscopy confirmed that several transient negative ion (TNI) states were formed upon electron attachment to isoxazole [7], to date, there are no data available on the subsequent fragmentation processes. This work describes a comparative study of DEA to isoxazole and its methylated derivatives, 3-methylisoxazole (H_5C_4NO) and 3,5-dimethylisoxazole (H_7C_4NO). For the purpose of further comparison, DEA to oxazole (H_3C_3NO), which is an isomer of isoxazole, and thiazole (H_3C_3NS) in which the oxygen is replaced by sulfur, were also investigated.

II. Experimental and Computational Methods

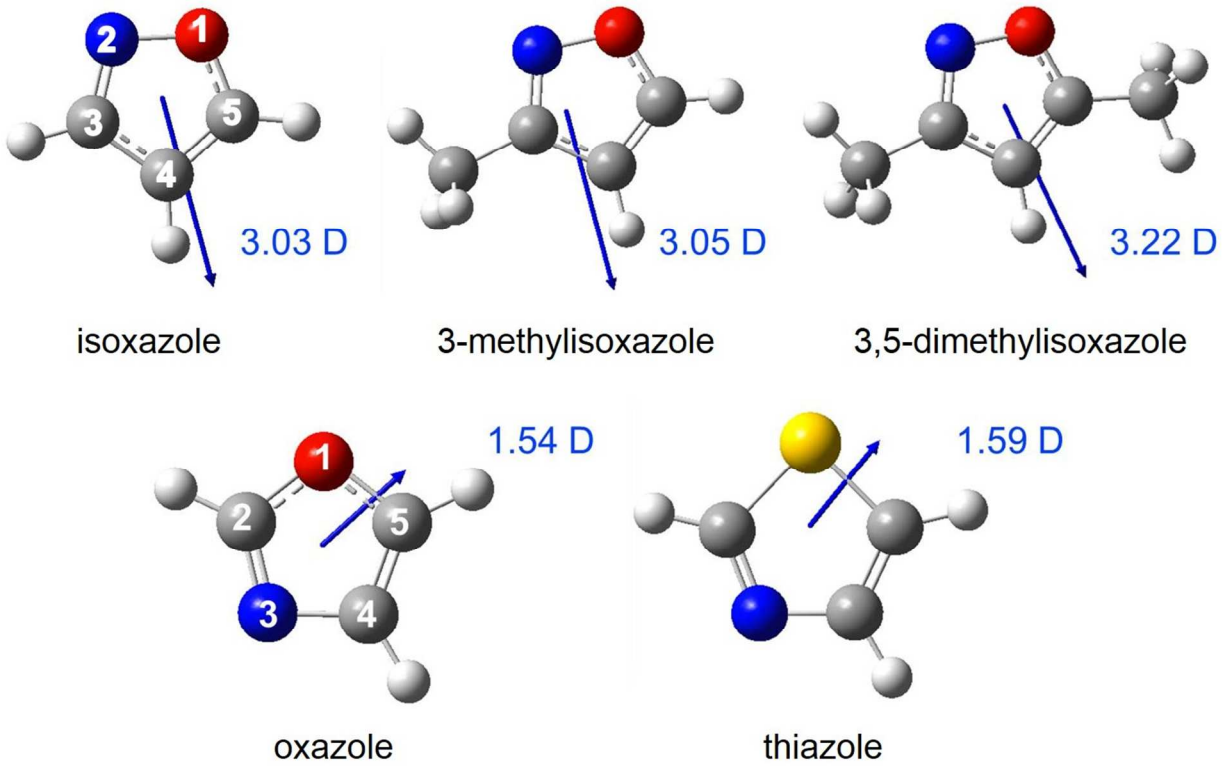

Figure 1. *Molecular structures of isoxazole, 3-methylisoxazole, 3,5-dimethylisoxazole, oxazole, and thiazole and dipole moments (Debye). The blue arrows indicate the dipole directions*.

The three samples used in this experiment, isoxazole (H_3C_3NO, 69 g/mol), 3-methylisoxazole (H_5C_4NO, 83 g/mol), and 3,5-dimethylisoxazole (H_7C_5NO, 97 g/mol), were commercial products with a stated purity of 99%, 98%, and 95%. The experiment was carried out at room temperature (25°C), at which all three samples remain in liquid form. At 25°C, the vapor pressure of the three samples was 51.7 ± 0.2 [18], 19.7 ± 0.2 [19], and 6.5 ± 0.3 mmHg [20], respectively. The liquid samples were contained in an evacuated glass vial and degassed with freeze-pump-thaw cycles to remove air and other possible gases. The experiment was conducted in a high vacuum chamber

with a base pressure of 10^{-10} mbar. When the gas phase DEA experiment was performed, vapor from the sample was introduced to the chamber through a leak valve that increased the chamber pressure to $1x10^{-6}$ mbar. The chamber was equipped with a quadrupole mass spectrometer (QMS: a 3F series model from Hiden Analytical, Inc.) that consisted of a built-in standard electron source component (a tungsten wire) affixed at the front end of the quadruple. Inside the vacuum chamber, the molecular beam was ejected from a metal tube with a diameter of 1 mm aimed at the front end of the QMS. The molecular beam entered the QMS and was crossed by the electron beam with an energy resolution of 0.3 eV emitted from the filament with an emission current of 1 μA. The resulting anions were guided into the triple-filter quadrupole system by several ion optical lenses. The ions with a selected mass-to-charge ratio (*m/z*) were counted with a Faraday detector while the electron energy was stepped in increments of 0.1 eV. The anion yield data were retrieved from the MASsoft interface provided by Hiden Analytical. In addition, to remove any background signal, the anion yield curves as a function of electron energy were taken from possible contaminants in the chamber and subtracted from the anion yield curves measured for the samples.

The standard enthalpy (heat) of reaction for each fragmentation pathway was calculated using the computational quantum chemistry package, Gaussian09 [21]. The enthalpy of reaction, ΔH^{θ}, at temperature (Θ) of 25°C was calculated as a subtraction of enthalpies of formation, $\Delta H^{\theta} = \sum H_f^{\theta}(products) - \sum H_f^{\theta}(reactants)$. The formation enthalpies for all of the molecules and radicals were calculated with a modified Complete Basis Set method, CBS-QB3, [22], [23], which is a composite procedure. Evidence has shown that CBS-QB3 is able to provide accurate results with very little penalty in computation time. For example, the calculation performed with

CBS-QB3 gives a mean absolute error of only 1.1 kcal/mol [39] on the G2/97 test set. Therefore, the enthalpy of reaction calculated is presumed to be reliable for each reaction pathway.

III. Results

3.1. DEA to isoxazole and its methylated isoxazoles

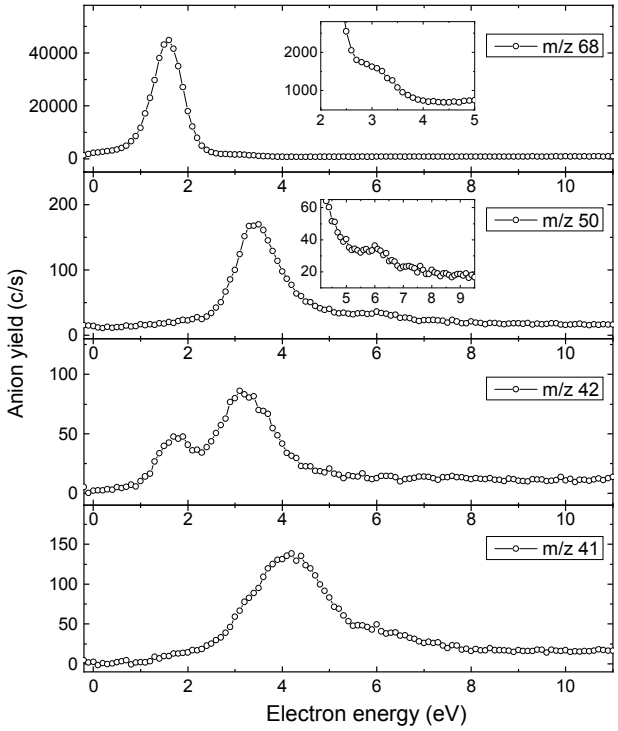

Figure 2. *Anion yield curves for fragments resulting from DEA to isoxazole as a function of electron energy.*

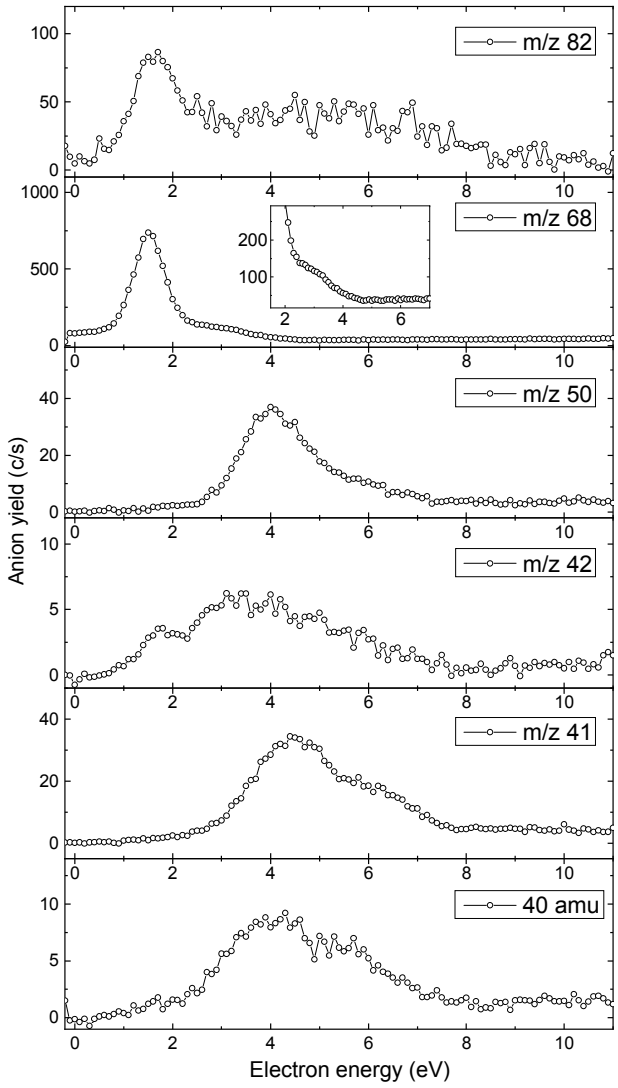

Figure 3. *Anion yield curves for fragments resulting from DEA to 3-methylisoxazole as a function of electron energy.*

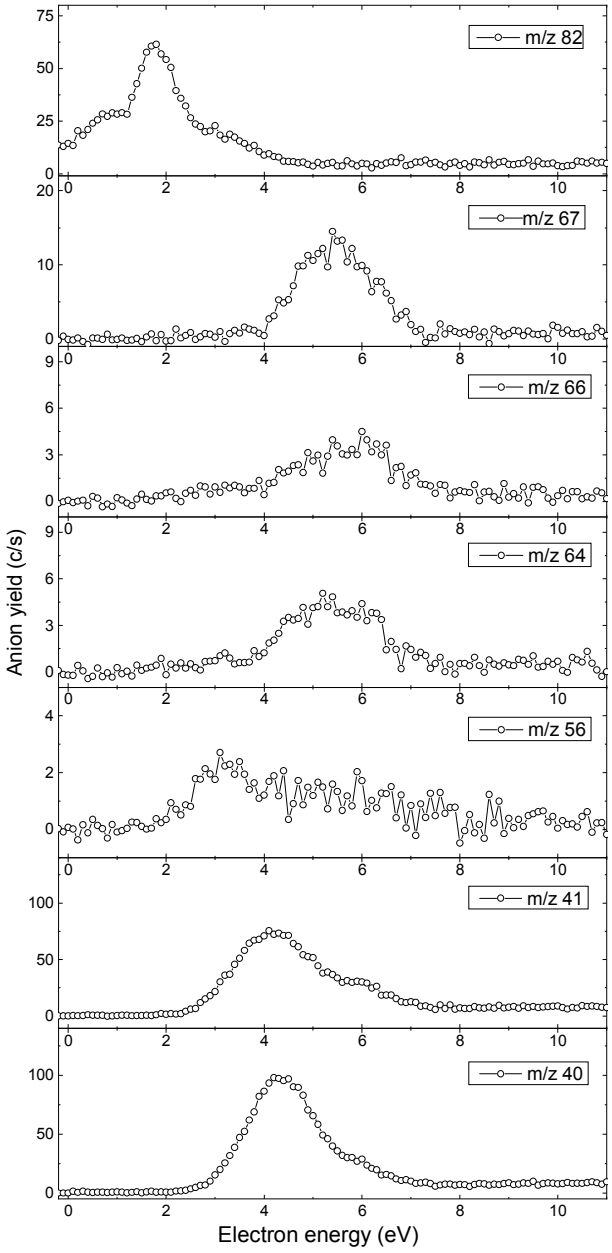

Figure 4. *Anion yield curves for fragments resulting from DEA to 3,5-dimethylisoxazole as a function of electron energy.*

As Figure 1 shows, isoxazole is a five-membered aromatic heterocyclic compound that is one of the aza-analogs of furan (C_4H_4O) in which a CH group is substituted by a nitrogen atom.

Because N has a relatively larger electronegativity than does CH, the substitution results in an increased distance in O(1)-N(2) and decreased distance in N(2)-C(3) in the ring [7]. Thus, the symmetry of the isoxazole is lowered from the C_{2v} point group symmetry of furan to C_s, and the dipole moment is increased from 0.66±0.01 to 2.95±0.04 D [40]. Here, we calculated the dipole moment of isoxazole as 3.03 D at the B3LYP/aug-cc-pVTZ level. Because 2.5 D is the threshold dipole for a neutral to bind an extra electron [41], the presence of the nitrogen atom enhances the electron-accepting property of isoxazole significantly.

Figure 2 presents the anion yield curves obtained from DEA to isoxazole. As a result of this process, anion yield curves with resonant features were observed for anions at *m/z* 68, 50, 42, and 41. As the figure shows, an intense resonance appeared at 1.6 eV in the anion yield curve at *m/z* 68, and as shown in the magnified inset, there was a smaller peak at approximately 3 eV. There were two maxima at 3.4 and 6 eV in the anion yield curve at *m/z* 50, and two resonant peaks were noted at 1.8 and 3.2 eV in the anion yield curve at *m/z* 42. The anion yield curve at *m/z* 41 had a major resonant peak at 4.2 eV and a smaller peak, indicated by the broad shoulder, at approximately 6 eV. These measurements can explain the total anion cross-section for DEA to isoxazole reported in an earlier paper by Walker et al. [42], according to whom the maxima of the total anion yield appeared at 1.5, 3.1, 4.5, and ~6-7 eV. By matching the positions of the peaks in Figure 2 with Walker *et al.*'s results, the 1.5 eV peak in the total anion yield curve was contributed by the 1.6 eV peak from the *m/z* 68 and 42 anion yield curves; both the peak at 3.1 eV in the *m/z* 68 anion yield curve and the 3.2 eV peak in the *m/z* 42 anion yield curve contributed to the 3.1 eV peak in the total anion yield curve. The weak 4.5 eV peak in the total anion yield curve [42] is actually a broad shoulder of the peak at 3 eV expanding from 3.5 to 5 eV, and therefore, it consists most likely of multiple peaks, *e.g.*, one at 3.4 eV from the *m/z* 50

signal and one at 4 eV from the *m/z* 41 signal. The 6 eV peak anion yield curves of the *m/z* 50 and 41 fragments observed correspond to the 6-7 eV peak in the total cross section. Table 1 summarizes all resonance positions observed in our study.

The mechanisms by which a neutral molecule traps an electron generally fall into two categories: shape resonance and core-excited resonance [1]. In shape resonance, the target molecule remains in its electronic ground state and the incoming electron is initially trapped by some form of potential barrier. In a core-excited resonance, the incoming electron first excites the target molecule to an excited energy level, and then becomes trapped by the excited molecule. In general, resonances at lower energies can be attributed to the TNI formed by shape resonance and at higher energies, to core-excited resonances if they are above the energy of the lowest excited state, which typically is approximately 4 eV [43]. The TNI then can eject the electron via autodetachment, or it dissociates into an anion, which can be detected directly in a typical DEA study, and neutral fragments, which can be detected by step-wise electron spectroscopy [44]. In the case of isoxazole, electron energy-loss (EEL) spectroscopy showed that the lowest-lying triplet states ($\pi \rightarrow \pi^*$ transition) appeared at 4.1 and 5.3 eV [42]. Further, the first photoabsorption region of isoxazole, accessing singlet excited states, appeared above 5.5 eV, with a maximum at approximately 6.0 eV [42]. Thus, the 6 eV resonance (*m/z* 50 and 41) observed in the anion yield curves can be $\pi \rightarrow \pi^*$ type core-excited resonance. Because the electron transmission experiment in isoxazole [7] showed that the two lowest-lying shape resonances were at 1.09 and 2.77 eV, and the calculation identified the three lowest resonances as π^*, π^* and σ^*_{ring} type [7], the resonances at approximately 1.6 eV (*m/z* 68 and 41) and ~3 eV (*m/z* 68 and 42) can be attributed to the lowest two π^* type shape resonances and the resonance at approximately 4 eV (*m/z* 50 and 41) to the σ^*_{ring} type shape resonance. This is quite different

from the case of furan, for which all of the major peaks induced by DEA are observed at approximately 6 eV and only a very small signal is detected below 4 eV for dehydrogenated furan, *i.e.*, $[furan\text{-}H]^-$ [11]. Replacing one carbon with nitrogen in the five-member ring structure increases the dipole moment significantly, and modifies the fragmentation pattern upon DEA significantly as well.

To identify the fragmentation pathways induced by LEEs, DEA to methylated isoxazoles, specifically 3-methylisoxazole and 3,5-dimethylisoxazole, was performed as well. The anion yield curves for 3-methylisoxazole and 3,5-dimethylisoxazole are shown in Figures 3 and 4. Among all of the fragments detected, the anion from isoxazole at *m/z* 68, which results from DEA-induced hydrogen loss, was the most abundant. There are three possible sites at which the hydrogen loss in isoxazole can occur, which are labeled 3, 4, and 5 in Figure 1. This fragmentation path can be expressed generally as reaction 1 and the three isomers of the dehydrogenated isoxazole anion, $H_2C_3NO^-$, are shown in Figure 5. Both methyl group (*m/z* 68) and hydrogen loss (*m/z* 82) were observed in the 3-methylisoxazole results. In the case of 3,5-dimethylisoxazole, no signals corresponding to hydrogen loss were observed, while the signals reflecting methyl-group loss were nearly an order of magnitude weaker than the corresponding ions in the singly-substituted compound. Hence, we concluded that the hydrogen loss induced by DEA occurs largely at site 3. The enthalpies of reaction for hydrogen loss calculated from sites 3, 4, and 5 were 0.04, 3.03, and 2.74 eV, respectively. Thus, only the hydrogen loss from site 3 requires an energy lower than 1.5 eV. This supports our conclusion that DEA-induced hydrogen loss in isoxazole occurs at site 3. In addition, our calculations indicated that the hydrogen loss from site 3 induces ring opening in the molecule, as shown in Figure 5.

$$e^- + H_3C_3NO \rightarrow H_2C_3NO^- + H\cdot \quad (1)$$

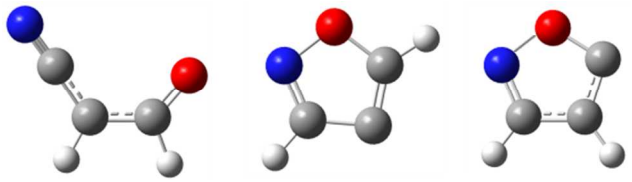

Figure 5. *Isomers of $H_2C_3NO^-$. From left to right, hydrogen loss occurs from site 3, 4, and 5, respectively.*

Based on the molecular weight, the anion at *m/z* 50 can be determined to be C_3N^-. The fragmentation process can be expressed as reactions 2a and 2b with reaction enthalpies of 2.1 and 2.7 eV, respectively. These values are consistent with the observations presented in Figure 2,that the threshold of the C_3N^- ion yield was located at ~ 2.7 eV, and had a maximum at 3.4 eV, and a weak maximum at 6 eV. The same anion C_3N^- also was detected in 3-methylisoxazole, in which the dominant resonant peak shifted to slightly higher energies centered at approximately 4 eV, with a broad shoulder in the region of 5 to 7 eV, as Figure 3 shows. Rather than anions at *m/z* 50, anions at *m/z* 64 were detected in 3,5-dimethylisoxazole, with a weak resonant peak spanning the range of 4 eV to 7 eV and centered at approximately 5 eV. This anion can be represented as $[H_2C\text{-}C_3N]^-$, a methylated analog of C_3N^-. Because in the case of 3-methylisoxazole, C_3N^- (*m/z* 50) was detected rather than $[H_2C\text{-}C_3N]^-$ (*m/z* 64), the formation of $[H_2C\text{-}C_3N]^-$ from 3,5-dimethylisoxazole must involve the scission of the C-C bond not at site 3, but at site 5. Another interesting observation was that the main resonance shifted gradually to higher energies, e.g., it was centered at 3.4 eV for isoxazole, while it was centered at 4 eV for 3-methylisoxazole, and the center was higher than 5 eV for 3,5-dimethylisoxazole. It seems that methylation elevates this specific initial resonant state's energy. The anions at *m/z* 66 and 67 amu from 3,5-dimethylisoxazole had anion yield curves with a profile similar to that at *m/z* 64, and exhibited a single peak spanning from 4 eV to 7 eV. This implies that they may have a molecular structure similar to that of $[H_2C\text{-}C_3N]^-$, and thereby, are represented by $H_4C_4N^-$ and $H_5C_4N^-$.

$$e^- + H_3C_3NO \rightarrow C_3N^- (\ \ ) + H_2O + H\cdot \quad (2a)$$

$$e^- + H_3C_3NO \rightarrow C_3N^- (\ \ ) + HO\cdot + H_2 \quad (2b)$$

The anion from isoxazole at *m/z* 42 can either be $H_2C_2O^-$ or CNO^-, as seen in reactions 3a-d. In the case of 3-methylisoxazole, an anion with the same mass (*m/z* 42) was observed with an anion yield curve that contained resonances in the same region, as seen in Figure 3. In this way, the hydrogen/methyl group at site 3 was removed when the anion at *m/z* 42 formed. Because an anion of *m/z* 56 was observed at approximately 3 eV in the 3,5-dimethylisoxazole result rather than a peak at *m/z* 42, the methyl group at site 5 was retained during this process. Therefore, it is impossible that the anion is $C(3)NO^-$. The calculation of the enthalpy of reaction showed that the formation of $C(5)ON^-$ (reaction 3d) requires an input of 6.9 eV. Thus, the anion at *m/z* 42 most likely has the structure of $H_2C_2O^-$. There are two possible isomers for this anion, $HCHCO^-$ and H_2CCO^-, as shown in reactions 3a and 3b. The corresponding enthalpy values required to form these two isomers were calculated as 0.7 eV (reaction 3a) and 1.8 eV (reaction 3b). These values are consistent with the experimental observation that the resonances that induced the formation of $H_2C_2O^-$ were at approximately 1.5 eV and 3 eV.

$$e^- + H_3C_3NO \rightarrow H_2CCO^- (\ \ ) + HCN \quad (3a)$$

$$e^- + H_3C_3NO \rightarrow HCHCO^- (\ \ ) + HCN \quad (3b)$$

$$e^- + H_3C_3NO \rightarrow C(3)NO^- (\ \ ) + HCH_2C \quad (3c)$$

$$e^- + H_3C_3NO \rightarrow C(5)ON^- (\ \ ) + HCH_2C \quad (3d)$$

Another major anionic fragment that resulted from DEA to isoxazole had a mass of *m/z* 41 and a main resonant peak in its anion yield curve centered at 4 eV and a weaker feature at approximately 6 eV. The corresponding fragments (*m/z* 41) in 3-methylisoxazole and 3,5-dimethylisoxazole both had a very similar profile in the anion yield curves, i.e., a major resonant peak at approximately 4 eV with a broad shoulder at higher energy. In addition, for both the methylated derivatives, an anion of *m/z* 40 was detected in the same energy region as that for the *m/z* 41 anion. The *m/z* 41 anion from isoxazole was assigned to HC_2O^- with the formation enthalpy calculated as 1.2 eV (reaction 4). The corresponding anions in 3-methylisoxazole and 3,5-dimethylisoxazole both occurred with the same mass (*m/z* 41), as seen in Figures 3 and 4. Thus, HC_2O^- is formed via N-O and C(3)-C(4) bond cleavage in the DEA process. Interestingly, the anion yield curve of *m/z* 40 was nearly identical to that of *m/z* 41 for both 3-methylisoxazole and 3,5-dimethylisoxazole, as shown in Figures 3 and 4. This anion either can be C_2O^-, caused by HC_2O^- losing an H atom, or $[CH_2\text{-}CN]^-$, the other possible anion formed by N-O and C(3)-C(4) bond cleavage. However, the *m/z* 40 anion was not observed in isoxazole, which indicates that it is not likely for HC_2O^- to lose an H atom to form C_2O^-. Therefore, we conjectured that the *m/z* 40 anion is $[CH_2\text{-}CN]^-$.

$$e^- + H_3C_3NO \rightarrow HC_2O^- (\text{}) + H_2NC \qquad (4)$$

From the discussion above, ring opening to isoxazole induced by DEA takes place via the three pathways shown in Figure 6. The dominant pathway is O-N bond cleavage, which results in the $[\text{isoxazole-H}]^-$ fragment. Cleavage of the O-N bond, the O-C bond, or a C-C bond can occur simultaneously, illustrated in the middle and right-hand side graphs in Figure 6. It is important to stress that all three pathways involve O-N bond cleavage.

Figure 6. ***Ring opening patterns induced by DEA to isoxazole.***

Table 1. The anionic fragments measured from DEA to isoxazole, 3-methylisoxazole, and 3,5-dimethylisoxazole.

Isoxazole			**3-methylisoxazole**			**3, 5-dimethylisoxazole**		
m/z (amu)	E_{max} (eV)	Anion	*m/z* (amu)	E_{max} (eV)	Anion	*m/z* (amu)	E_{max} (eV)	Anion
			82	1.7	$H_4C_4NO^-$	82	1.7	$H_4C_4NO^-$
68	1.6, 3	$H_2C_3NO^-$	68	1.5, 3	$H_2C_3NO^-$			
						67	5.4	$H_5C_4N^-$
						66	5.8	$H_4C_4N^-$
50	3.4, 6	C_3N^-	50	4	C_3N^-	64	5.5	$H_2C_4N^-$
42	1.8, 3.2	$H_2C_2O^-$	42	1.8, 3.5	$H_2C_2O^-$	56	3.2	$H_4C_3O^-$
41	4.2, 6.0	HC_2O^-	41	4.5, 6.0	HC_2O^-	41	4.2	HC_2O^-
			40	4.2, 6.0	$H_2C_2N^-$	40	4.3	$H_2C_2N^-$

3.2. DEA to oxazole and thiazole

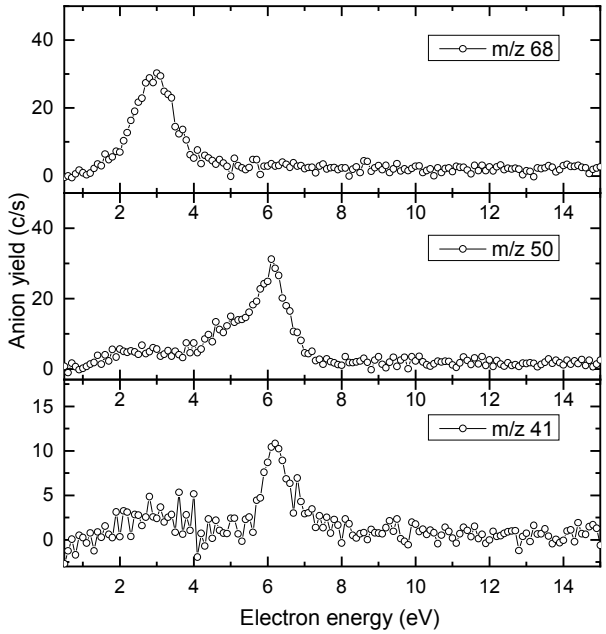

Figure 7. *Anion yield curves for fragments resulting from DEA to oxazole as a function of electron energy.*

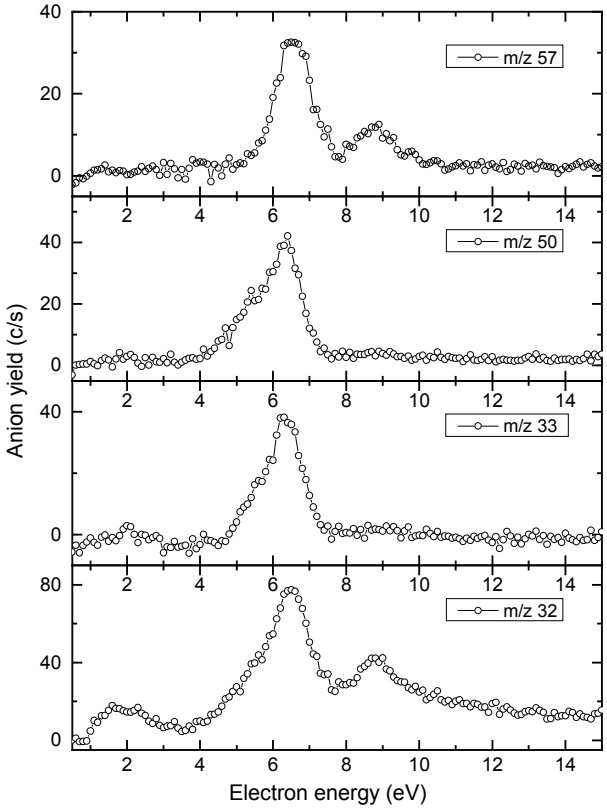

Figure 8. *Anion yield curves for fragments resulting from DEA to thiazole as a function of electron energy.*

The major anion yield curves that resulted from DEA to oxazole are shown in Figure 7. Compared to isoxazole's anion yield curves, the intensity of the resonance peaks from oxazole generally was one order of magnitude lower (all measurements were carried out at 10^{-6} mbar with the same experimental settings). This phenomenon can be attributed to oxazole's weak dipole moment, which, according to our calculations, was approximately twice as small as that of isoxazole (Figure 1). The resonance peak at 3 eV for the anion at *m/z* 68 can be assigned to shape

resonance, as the typical threshold from core-excited resonance is approximately 4 eV. In addition, the lowest core-excited state for oxazole reported by Palmer and co-workers [45] through EEL spectroscopy is a $^3\pi\pi^*$ state at 4.6 eV. The anion yield curves for *m/z* 50 and *m/z* 41 both displayed a major resonance peak at approximately 6 eV, which corresponded to the 6 eV resonance peak in oxazole's EEL spectrum. The broad shoulder on the lower-energy side of the 6 eV peak in the anion yield curve for *m/z* 50, which extended from 4 to 5.5 eV, was consistent with the 4.6 eV resonance seen in oxazole's EEL spectrum [45]. In contrast, the EEL spectrum exhibited an additional structure with a major peak at 1.4 eV that arose from resonant vibrational excitation of the molecule via a shape resonance, while in this DEA study, no resonances were observed below 3 eV. Figure 8 shows the anion yield curves for thiazole. Resonance signals were observed in the anion yield curves of *m/z* 57, *m/z* 50, *m/z* 33, and *m/z* 32. All of the anion yield curves had a major peak with a maximum at 6.5 eV and a broad shoulder with low energies that appeared at 4 eV for *m/z* 50, *m/z* 33, and *m/z* 32. A previous photoabsorption study of thiazole showed that the two lowest bands corresponding to the two lowest excited states of thiazole spanned the region from 4 to 6.5 eV [46]. Therefore, the weak signal in the anion yield curve for *m/z* 50 and *m/z* 32 can be attributed to the two lowest core-excited resonance anion states. The anion yield curves demonstrated a major resonance peak at 6.5 eV and a smaller signal at 9 eV for the *m/z* 57 and *m/z* 32 anions from thiazole.

In our study, DEA-induced hydrogen loss also was observed in oxazole, although the signal was much weaker than was that for isoxazole (two orders of magnitude lower). The enthalpy change was calculated for all three possible pathways. The hydrogen loss from sites 2, 4, and 5 that produced the three $[\text{oxazole-H}]^-$ (*m/z* 68) isomers shown in 9, required an energy of 1.6, 2.1, and 1.7 eV, respectively. All three of these values were lower than 3 eV, the energy at which the

resonance peak is located. Therefore, all three pathways may contribute to the generation of a dehydrogenated oxazole anion. In addition, our calculations indicated that the ring structure should be maintained during this process. We did not observe C-H bond dissociation in DEA to thiazole. This could be explained by the reaction enthalpies that are required to create dehydrogenated thiazoles, which we calculated were 4.9, 5.0, and 5.2 eV for C-H bond cleavage from sites 2, 4, and 5 on the thiazole ring. These values are much higher than the energy required to create singly dehydrogenated oxazole anions.

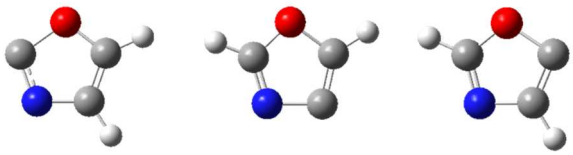

Figure 9. *Dehydrogenated oxazole anion created from DEA-induced C-H bond cleavage. From left to right, the hydrogen loss occurs at sites 2, 4 and 5.*

An anion signal at *m/z* 50 (C_3N^-) was observed in both oxazole and thiazole. The two anion yield curves bore very similar profiles, with a dominant peak centered at 6 eV. We calculated the reaction enthalpies required to produce this anion from oxazole (reaction 5) and from thiazole (reaction 6) as 3.2 and 4.9 eV, respectively. All of these values were below the peak centered at 6 eV. Interestingly, we also observed this anion from isoxazole, but it formed at a lower energy and, as shown in reaction 2, had a different structure.

$$e^- + H_3C_3NO \rightarrow C_2NC^- (\text{ 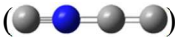 }) + H_2O + H\cdot \quad (5)$$

$$e^- + H_3C_3NS \rightarrow C_2NC^- (\text{}) + H_2S + H\cdot \quad (6)$$

The anion *m/z* 41 from DEA to oxazole can be attributed to HC_2O^- or $H_3C_2N^-$. The enthalpies calculated to produce these two anions were 0.9 eV (reaction 7a) and 0.5 eV (reaction 7b) both

of which were lower than the resonance region. However, in the DEA to thiazole, rather than a *m/z* 41 anion, a *m/z* 57 anion signal (HC_2S^-) was observed, which had the same structure as that in reaction 7a, but the oxygen in HC_2O^- was substituted by sulfur (reaction 8). Therefore, it is more plausible that the *m/z* 41 anion from oxazole is HC_2O^-.

$$e^- + H_3C_3NO \rightarrow CHCO^- (\text{ 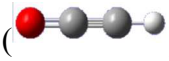 }) + NCH_2 \quad (7a)$$

$$e^- + H_3C_3NO \rightarrow CH_2CHN^- (\text{ 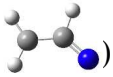 }) + CO \quad (7b)$$

$$e^- + H_3C_3NS \rightarrow CHCS^- (\text{  }) + NCH_2 \quad (8)$$

As Figure 8 illustrates, in DEA to thiazole, both anions of *m/z* 32 (S^-) and *m/z* 33 (HS^-) were observed. The anion yield curve of S^- was similar in profile to that of the *m/z* 57 anion (HC_2S^-), with a double peaked shape with maxima at 6.5 and 9 eV. Thus, S^- can be considered a product of HC_2S^- via further dissociation accomplished by breaking the S-C bond. Production of HS^- needs to undergo a ring fragmentation process by breaking the C(2)-S and C(5)-S bonds, which also can lead to C_3N^- production. This suggests an explanation for the nearly identical anion yield curves of HS^- (*m/z* 33) and C_3N^- (*m/z* 50). A previous study of DEA to nucleobases showed delayed (metastable) fragmentation upon electron attachment and subsequent ring opening [47]. Such a delayed decomposition can be caused by accommodation of a substantial amount of the internal energy in a polyatomic molecule.

Based on the analysis above, the ring opening patterns in oxazole and thiazole induced by DEA can be summarized as in Figure 10. There are two pathways through which DEA to these five-membered rings destroys the ring structure for both molecules: 1) by cleaving the two O/S-C bonds, and 2) by cleaving the O/S-C(2) and N-C(4) bonds. Cleavage of the O-C(2) bond was involved in both of the ring openings in oxazole, indicating that the O-C(2) bond is the weakest

one on the oxazole ring. This is consistent with Culberson at el.'s findings, in which photodetachment of the oxazole anion led to ring opening by breaking the same O-C bond [48].

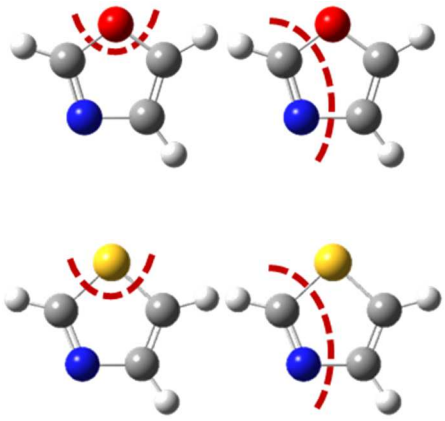

Figure 10. *Ring opening patterns induced by DEA for oxazole (top row) and thiazole (bottom) row.*

IV. Conclusion

In this work, we measured the anion yield curve for each anion and identified several resonant states that resulted in the dissociation of isoxazole. The lowest three shape resonances (below 5 eV) were found to initiate isoxazole dissociation by inducing N-O, C(3)-C(4), and C-O bond cleavage. In particular, the most dominant fragmentation pathway that formed $[\text{isoxazole-H}]^-$ via hydrogen loss at site 3 was initiated by the lowest shape resonance state. The lowest core-excited resonance at approximately 6 eV also induced dissociation, but with a much lower intensity than did the shape resonance below 5 eV. This is quite different from the case of furan, in which the DEA-induced fragmentation largely is initiated via core-excited resonances. Therefore, in furan, substituting the C(2)H group with nitrogen enhanced the molecule's electron scavenging ability in the lower energy region (<5 eV) greatly, and thus, the subsequent dissociation behavior.

Our comparative study of isoxazole, 3-methylisoxazole, and 3,5-dimethylisoxazole elucidated the fragmentation pathway that leads to each anion product induced by DEA. With the help of quantum chemistry calculations, each reaction pathway also was rationalized theoretically by calculating the enthalpies of reaction. According to the discussion in this paper, all DEA-induced fragmentation pathways in isoxazoles involved ring opening via N-O bond cleavage. This is consistent with the thermolysis behavior of isoxazole [49],[50] that initiates with N-O bond cleavage and leads ultimately to the yield of nitriles observed. Upon DEA, oxazole and thiazole also exhibited ring opening. The major pathway by which the oxazole ring was broken was by cleaving the C(2)-O(1) and C(5)-O(1) bonds, which led to the production of CNC_2^-, and cleaving the C(2)-N(3) and C(5)-O(1) bonds, which led to the production of HC_2O^-. The corresponding fragmentation patterns also were found in thiazole. Although we detected the dehydrogenated oxazole anion in the experiment, the signal was much lower than was that of the dehydrogenated isoxazole anion. In addition, the calculation indicated that this process did not damage the ring structure in oxazole. Therefore, we concluded that the N-O bond on the five-membered ring structure in isoxazole is highly susceptible to DEA.

For azole compounds' diverse applications in area such as pharmaceutics, agrochemistry, etc., the ring opening patterns have been the subject of many studies. The tendency for ring opening via N-O bond scission in the biotransformation process accounts for the function of isoxazole-containing compounds [15],[16]. Therefore, the demonstration in this work of extensive ring opening upon DEA and the detailed examination of consequential products can be valuable in fields such as pharmaceutical research and engineering.

Acknowledgments

The work was supported by the U.S. Department of Energy Office of Science, Office of Basic Energy Sciences under Award Number DE-FC02-04ER15533. This is contribution number NDRL 5209 from the Notre Dame Radiation Laboratory.

References

[1] J. Gorfinkiel and S. Ptasinska, *J. Phys. B*, 2017, **50**, 182001.
[2] B. Boudaïffa, P. Cloutier, D. Hunting, M.A. Huels and L. Sanche, *Science*, 2000, **287**, 1658.
[3] M. A. Huels, B. Boudaïffa, P. Cloutier, D. Hunting and L. Sanche, *J. Am. Chem. Soc.*, 2003, **125**, 4467.
[4] H.-P. Fenzlaff and E. Illenberger, *Int. J. Mass Spectrom. Ion Process.*, 1984, **59**, 185.
[5] I. Linert, I. Lachowicz, T.J. Wasowicz and M. Zubek, *Chem. Phys. Lett.*, 2010, **498**, 27.
[6] I. Linert and M. Zubek, *Phys. Rev. A*, 2012, **86**, 022708.
[7] A. Modelli and P. D. Burrow, *J. Phys. Chem. A*, 2004, **108**, 5721.
[8] R.F. da Costa, M.T. do N. Varella, M.A.P. Lima and M.H.F. Bettega, *J. Chem. Phys.*, 2013, **138**, 194306.
[9] M.V. Muftakhov, N.L. Asfandiarov and V.I. Khvostenko, *J. Electron Spectros. Relat. Phenomena*, 1994, **69**, 165.
[10] M. Vinodkumar, H. Desai and P.C. Vinodkumar, *RSC Adv.*, 2015, **5**, 24564.
[11] P. Sulzer, S. Ptasinska, F. Zappa, B. Mielewska, A.R. Milosavljevic, P. Scheier, T.D. Märk, I. Bald, S. Gohlke, M.A. Huels and E. Illenberger, *J. Chem. Phys.*, 2006, **125**, 44304.
[12] G.A. Patani and E.J. LaVoie, *Chem. Rev.*, 1996, **96**, 3147.
[13] J. Ashby and B.M. Elliott, *Comprehensive Heterocyclic Chemistry*, Vol **1**, A. R. Katritzky and C. W. Rees, Eds. Pergamon, Oxford, 1984, 111.
[14] S. D. Nelson, *J. Med. Chem.*, 1982, **25**, 753.
[15] J. Yu, J.J. Folmer, V. Hoesch, J. Doherty, J.B. Campbell and D. Burdette, *Drug Metab. Dispos.*, 2011, **39**, 302.
[16] B. Rozman, *Clin. Pharmacokinet.*, 2002, **41**, 421.
[17] D.K. Dalvie, A.S. Kalgutkar, S.C. Khojasteh-Bakht, R.S. Obach, J.P. O'Donnell, *Chem. Res. Toxicol.*, 2002, **15**, 269.
[18] "isoxazole | C3H3NO | ChemSpider." [Online]. Available: http://www.chemspider.com/Chemical-Structure.8897.html.
[19] "3-methylisoxazole | C4H5NO | ChemSpider." [Online]. Available: http://www.chemspider.com/Chemical-Structure.86744.html. [Accessed: 30-Jan-2017].
[20] "3,5-Dimethylisoxazole | C5H7NO | ChemSpider." [Online]. Available: http://www.chemspider.com/Chemical-Structure.8953.html. [Accessed: 30-Jan-2017].
[21] M.J. Frisch, G.W. Trucks, H.B. Schlegel, G.E. Scuseria, M.A. Robb, J.R. Cheeseman, G. Scalmani, V. Barone, B. Mennucci, G.A. Petersson, H. Nakatsuji, M. Caricato, X. Li, H.P.

Hratchian, A.F. Izmaylov, J. Bloino, G. Zheng, J.L. Sonnenberg, M. Hada, M. Ehara, K. Toyota, R. Fukuda, J. Hasegawa, M. Ishida, T. Nakajima, Y. Honda, O. Kitao, H. Nakai, T. Vreven, J.A. Montgomery Jr., J.E. Peralta, F. Ogliaro, M. Bearpark, J.J. Heyd, E. Brothers, K.N. Kudin, V.N. Staroverov, R. Kobayashi, J. Normand, K. Raghavachari, A. Rendell, J.C. Burant, S.S. Iyengar, J. Tomasi, M. Cossi, N. Rega, J.M. Millam, M. Klene, J.E. Knox, J.B. Cross, V. Bakken, C. Adamo, J. Jaramillo, R. Gomperts, R.E. Stratmann, O. Yazyev, A.J. Austin, R. Cammi, C. Pomelli, J.W. Ochterski, R.L. Martin, K. Morokuma, V.G. Zakrzewski, G.A. Voth, P. Salvador, J.J. Dannenberg, S. Dapprich, A.D. Daniels, Ö. Farkas, J.B. Foresman, J.V Ortiz, J. Cioslowski and D.J. Fox, *Gaussian 09, Revision E.01*. Wallingford, CT: Gaussian Inc., 2009.

[22] J. . Montgomery, M.J. Frisch, J.W. Ochterski and G.A. Petersson, *J. Chem. Phys.*, 1999, **110**, 2822.

[23] J.A. Montgomery, M.J. Frisch, J.W. Ochterski and G. A. Petersson, *J. Chem. Phys.*, 2000, **112**, 6532.

[24] A.D. Becke, *J. Chem. Phys.*, 1993, **98**, 5648.

[25] G.A. Petersson, T.G. Tensfeldt and J.A. Montgomery, *J. Chem. Phys.*, 1991, **94**, 6091.

[26] Č. Jiří, *Advances in Chemical Physics: Correlation Effects in Atoms and Molecules*, vol. 14, Hoboken, NJ, USA: John Wiley & Sons, Inc., 2007, pp. 35–89.

[27] G.D. Purvis and R.J. Bartlett, *J. Chem. Phys.*, 1982, **76**, 1910.

[28] G.E. Scuseria, C.L. Janssen and H.F. Schaefer, *J. Chem. Phys.*, 1988, **89**, 7382.

[29] G.E. Scuseria and H.F. Schaefer, *J. Chem. Phys.*, 1989, **90**, 3700.

[30] G.A. Petersson, A. Bennett, T.G. Tensfeldt, M.A. Al-Laham, W.A. Shirley and J. Mantzaris, *J. Chem. Phys.*, 1988, **89**, 2193.

[31] G.A. Petersson and M.A. Al-Laham, *J. Chem. Phys.*, 1991, **94**, 6081.

[32] R. Krishnan and J.A. Pople, *Int. J. Quantum Chem.*, 1978, **14**, 91.

[33] R. Krishnan, M.J. Frisch and J.A. Pople, *J. Chem. Phys.*, 1980, **72**, 4244.

[34] M. Head-Gordon, J.A. Pople and M.J. Frisch, *Chem. Phys. Lett.*, 1988, **153**, 503.

[35] S. Sæbø and J. Almlöf, *Chem. Phys. Lett.*, 1989, **154**, 83.

[36] M.J. Frisch, M. Head-Gordon and J.A. Pople, *Chem. Phys. Lett.*, 1990, **166**, 281.

[37] M.J. Frisch, M. Head-Gordon and J.A. Pople, *Chem. Phys. Lett.*, 1990, **166**, 275.

[38] M. Head-Gordon and T. Head-Gordon, *Chem. Phys. Lett.*, 1994, **220**, 122.

[39] J.A. Montgomery, M.J. Frisch, J.W. Ochterski and G.A. Petersson, *J. Chem. Phys.*, 2000, **112**, 6532.

[40] D.R. Lide, *CRC handbook of chemistry and physics: a ready-reference book of chemical and physical data*. CRC Press, 2004.

[41] K.D. Jordan, V.K. Voora and J. Simons, *Theor. Chem. Acc.*, 2014, **133**, 1.

[42] I.C. Walker, M.H. Palmer, J. Delwiche, S.V Hoffmann, P.M. Limao-Vieira, N.J. Mason, M.F. Guest, M.-J. Hubin-Franskin, J. Heinesch and A. Giuliani, *Chem. Phys.*, 2004, **297**, 289.

[43] G.J. Schulz, *Rev. Mod. Phys.*, 1973, **45**, 423.

[44] Z. Li, A.R. Milosavljevic, I. Carmichael and S. Ptasinska, *Phys. Rev. Lett.*, 2017, **119**, 053402.

[45] M.H. Palmer, G. Ganzenmüller and I.C. Walker, *Chem. Phys.*, 2007, **334**, 154.

[46] M.H. Palmer, *Chem. Phys.*, 2008, **344**, 21.

[47] F. Ferreira da Silva, C. Matias, D. Almeida, G. García, O. Ingólfsson, H. Dögg Flosadóttir, B. Ómarsson, S. Ptasinska, B. Puschnigg, P. Scheier, P. Limão-Vieira and S. Denifl, *J. Am.*

Soc. Mass Spec., 2013, **24**, 1787–97, (2013).
[48] L.M. Culberson, A.A. Wallace, C.C. Blackstone, D. Khuseynov and A. Sanov, *Phys. Chem. Chem. Phys.*, 2014, **16**, 3964.
[49] P. Grünanger and P. Vita-Finzi, Eds., "Isoxazoles," in *Chemistry of Heterocyclic Compounds*, vol. 47, Hoboken, NJ, USA: John Wiley & Sons, Inc., 1991, p. 1.
[50] T.M.V.D. Pinho e Melo, *Curr. Org. Chem.*, 2005, **9**, 925.

Table of contents:

Ring opening in five-membered rings induced by gentle impact of low energy electrons.